China Petroleum Processing and Petrochemical Technology

Catalyst Research Volume 23, Issue 2, September 2023 Pp. 614-630

DESIGN OF THE COMPACT FREQUENCY RECONFIGURABLE HEXA-BAND ANTENNA WITH SMALL FREQUENCY RATIOS

Koduri Sreelakshmi

Department of ECE, Andhra University College of Engineering (A), Andhra University, Vishakhapatnam, India.

ABSTRACT The development and evaluation of a compact hexa-band antenna employing the PIN diode to realize frequency reconfigurable characteristics is investigated in this article. The presented antenna is backed by a ground plane and printed on top of a 1.6 mm thicker FR4 substrate. The antenna size is very compact (24 mm × 19 mm × 1.6 mm), and can be readily incorporated with many other RF front-end circuits. The presented antenna consists of a rectangular microstrip patch antenna, F-shaped monopole, Z shaped monopole, two T shaped monopoles and inverted L-shaped monopole. The investigated antenna realizes hexa/Triple band characteristics by turning ON/OFF the PIN diode positioned between the F shaped monopole and metal strip. While in OFF state, the investigated antenna covers 6 unique frequencies 2.3 GHz (LTE Band 30), 2.5 GHz (LTE Band 53), 3.35 GHz (LTE Band 52), 4.4 GHz (Radio altimeter), 5.3 GHz (U-NII-2A) and 5.6 GHz (U-NII-2C) and in ON state, the antenna covers 3 unique frequencies 4.35 GHz (Radio altimeter), 5.25 GHz (U-NII-1 & U-NII-2A), and 5.65 GHz (U-NII-2C) for wireless applications. The investigated antenna demonstrates very modest frequency ratios of 1.086/1.34/1.31/1.20/1.05 between two successive bands. The measurements demonstrate that the designed antenna has unidirectional radiation characteristics with 1 to 6 dBi gain. The investigated design's simulated and measured results are compared, and they demonstrate good agreement.

INDEX TERMS Hexaband, LTE, Radio altimeter, Reconfigurable, U-NII-2A

I. INTRODUCTION

With the continuous growth in wireless communication, contemporary transceiver systems enable a variety of services such as multimedia, data, telephony, GPS, internet access, and Bluetooth, among others. Antennas operating at a single frequency band [1] are limited to use for one service only. As a result, more antennas are required for applications that require several radios. More number of antennas result in large space consumption, interference between adjacent antenna elements, huge installation cost and complex hardware platform. To overcome this drawback, compact multiband antennas are required. These antennas serve as a replacement for multiple separate antennas, reducing the size of operating equipment. One valid strategy for meeting the demand for multiband operation is to construct an ultra-wideband or even broadband antennas to accommodate all applications. But the latter may not be appropriate wherever communications are not needed at specific frequencies, demanding the elimination of interfering oscillations. Multiband antennas are required in this scenario to avoid producing or detecting interference. Numerous researchers have attempted to develop such antennas that are suitable for multiband

operations. [2-3]. When developing a multiband antenna, achieving small frequency ratios between two successive resonant frequencies is critical. Another appealing aspect of a multiband antenna is its small frequency ratio between two successive resonant bands, which prevents the system from wasting bandwidth and reduces interference between the two bands. Numerous antenna configurations with a low frequency ratio have been proposed [4–7]. A novel shaped penta resonant patch antenna is reported in [8]. A penta resonant single layer antenna for vehicular communication is reported in [9]. A hexa band antenna with novel shaped patch is reported in [10]. A novel planar multislot–multiband planar antenna [11]. A novel multiband unidirectional patch antenna with integrated resonators is investigated in [12]. A compact triple band irregular shaped patch antenna loaded with asymmetric slits is reported in [13]. A rectangular slotted patch antenna for pentaband operation is reported in [14]. A compact nested rectangular loop penta resonant antenna fed with coplanar waveguide is reported in [15]. A hexaband patch antenna with novel design is proposed in [16] But, there are some drawbacks of multiband antennas with small frequency ratios which are reported in [4-16]. Nevertheless, these multiband antennas [4-16] transmit all resonances irrespective of customer requirement, implying that they are not reconfigurable. Instead, tuning a multiband antenna at the desired frequency is not possible. Hence, employing frequency reconfigurability to existing multiband antennas can enhance the functioning of them. Moreover, the frequency reconfigurable antenna provides outstanding out-of-band noise rejection, which greatly decreases the front-end circuitry's filtering demands. [17]. Researchers have worked hard to develop frequency reconfigurable antennas for a variety of applications. A compact reconfigurable pattern hexa-band antenna is presented in [18], a planar low profile antenna with pattern and frequency reconfigurability is designed in [19], a multiband antenna with the compact size of $50 \times 45 \times 1.6$ mm^3 is investigated in [20], a compact reconfigurable frequency multimode, multiband antenna for diverse wireless applications is presented in [**21**], a printed low-profile, antenna with frequency and pattern reconfigurability is presented in [22], a low-profile, compact size, inexpensive, and easily integrable frequency reconfigurable antenna system is proposed in [23] and a compact frequency reconfigurable quad-band antenna was presented and investigated in [24]. However, despite being reconfigurable, these antennas [18-24] have large dimensions and only a few operational bands, which restricts their applications in contemporary RF front-ends where there is a limited amount of space for the antennas. Additionally, a few of these antennas [18–24] used numerous bias lines, lumped components, and more PIN diodes to tune the operating states, which complicated the antenna structure and created additional integration and cost challenges.

In this paper, a compact GACS-fed frequency reconfigurable hexa-band antenna is investigated. The investigated design achieves frequency band reconfigurability by incorporating a switching element PIN diode between the F-shaped monopole and a rectangular metal strip. The investigated antenna is compatible with over six various wireless standards, which include, LTE Band 30, 53, 52, radio altimeter, U-NII-2A and U-NII-2C. The remainder of the manuscript is organized as follows: Section II presents the working principle, detailed design strategy, and evolution process. Section III presents the explanation about electrical model and biasing circuit of the PIN diode

Catalyst Research Volume 23, Issue 2, September 2023 Pp. 614-630

which is employed to achieve frequency reconfigurability. Section IV depicts the fabricated prototype of the investigated antenna, as well as the results of the simulated and measured reflection coefficient, gain, and radiation patterns. Conclusions are provided in Section V.

II. ANTENNA DESIGN AND CONFIGURATION METHODOLOGY

A. ANTENNA GEOMETRY

Fig. 1(a)–(b) depicts the top, and side views of the investigated frequency reconfigurable hexaband antenna, respectively. An inexpensive and commercially available material called FR4, with thickness, relative permittivity (ε_r), and tangent loss (tan δ), of 1.6 mm, 4.4, and 0.024, respectively, is utilized for the substrate of the presented hexaband antenna.

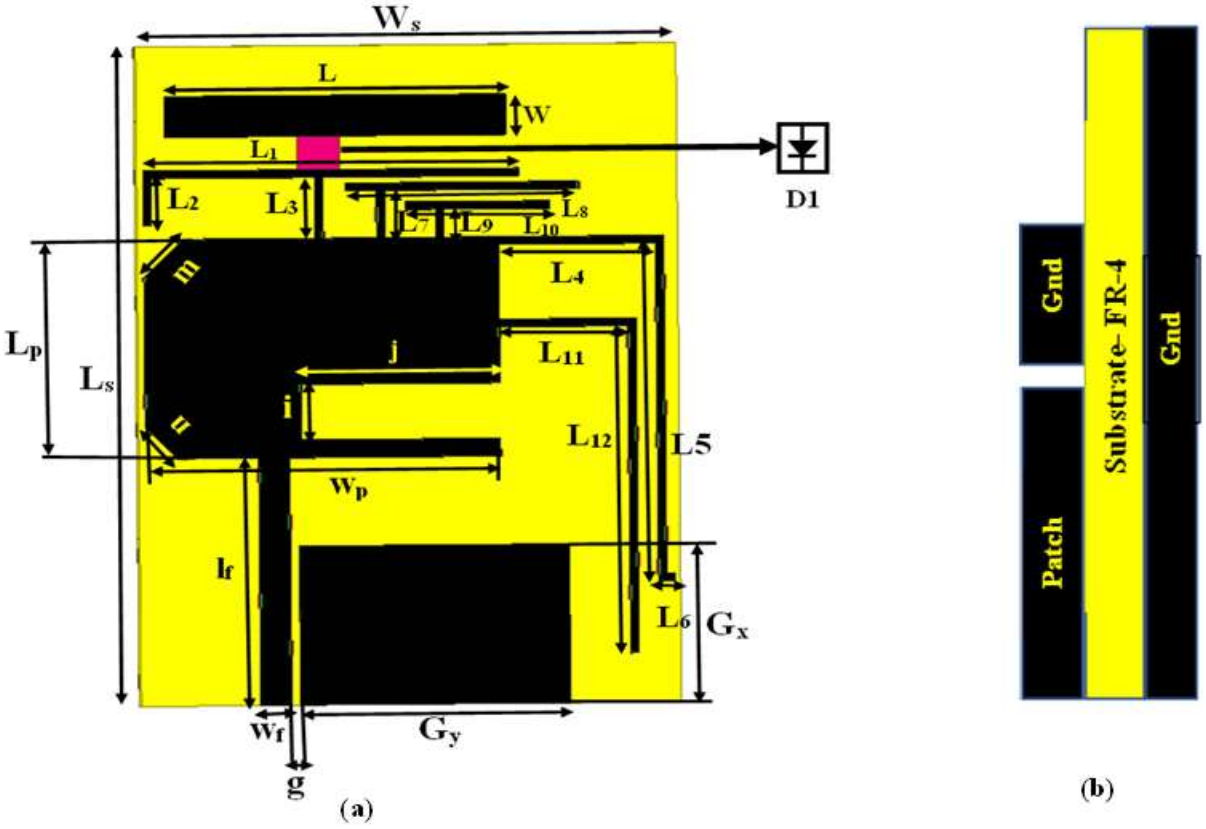

FIGURE 1. Schematic layout of the presented antenna a) Front view and b) Side view

The presented hexaband antenna has compact size of 24 mm × 19 mm. The presented antenna is fed via a 50 GACS feedline with a 1.1 mm signal strip and a 0.3 mm gap distance between the asymmetric ground plane and signal strip. The designed antenna is composed of a rectangular microstrip patch antenna connected to GACS feed line. To enhance impedance matching, the patch's edges are trimmed on the left side, and a U-shaped slot is created on the patch's right side. An F-shaped monopole, Z shaped monopole, two T shaped monopoles and inverted L-shaped monopole that are attached to a rectangular microstrip patch antenna. To achieve frequency reconfigurability an RF PIN diode switch is incorporated between the F- shaped monopole and

metal strip of length L and width W. The investigated antenna is designed with the help of high frequency structure simulation software (HFSS). Table 1 depicts the optimized dimensions.

TABLE I
THE INVESTIGATED ANTENNA'S PRECISE DIMENSIONS

Parameter	Value (mm)	Parameter	Value (mm)
L_s	24	w_p	14
W_s	19	i	2
G_x	5.8	j	7
G_y	9.5	m	1.97
l_f	9	n	1.63
w_f	1.1	L_1	13.05
g	0.3	L_2	2
L_p	10	L_3	2.5
L_4	5.5	L_7	1.7
L_5	12.61	L_8	8.2
L_6	0.3	L_9	1
L_{10}	5.1	L_{11}	4.5
L_{12}	12.2	L	12
W	1.5		

B. DESIGN EVOLUTION

The step wise development of the presented design is depicted in five consecutive stages as shown in Fig. 2. In the initial step (Antenna I) antenna consists of rectangular microstrip patch antenna connected to GACS feed line.To enhance impedance matching, the patch's edges are trimmed on the left side, and a U-shaped slot is created on the patch's right side. The width and length of the basic rectangular patch antenna can be calculated by the following design equations [1].Antenna-I is designed to operate at $f_{U\text{-}NII\text{-}2C}$ = 5.68 GHz as its primary fundamental frequency.

The width (W_p) of Antenna I is determined as

$$W_p = \frac{c}{2f_{U-NII-2C}}\sqrt{\frac{2}{\varepsilon_r+1}}$$

Where c, ε_r and f_r, are the speed of light in vaccum, relative permittivity, and resonant frequency, respectively.

The Length (L_p) of Antenna I is determined as,

$$L_p = \frac{c}{2f_{U-NII-2C}\sqrt{\varepsilon_{reff}}} - 2\Delta L$$

where effective permittivity ε_{reff} is given by

$$\varepsilon_{reff} = \frac{\varepsilon_r+1}{2} + \frac{\varepsilon_r-1}{2\sqrt{1+\frac{12h}{W_p}}}$$

and

$$\Delta L = 0.412h\frac{\left(\varepsilon_{reff}+0.3\right)\left(\frac{W_p}{h}+0.264\right)}{\left(\varepsilon_{reff}-0.258\right)\left(\frac{W_p}{h}+0.8\right)}$$

where h is the thickness of substrate.

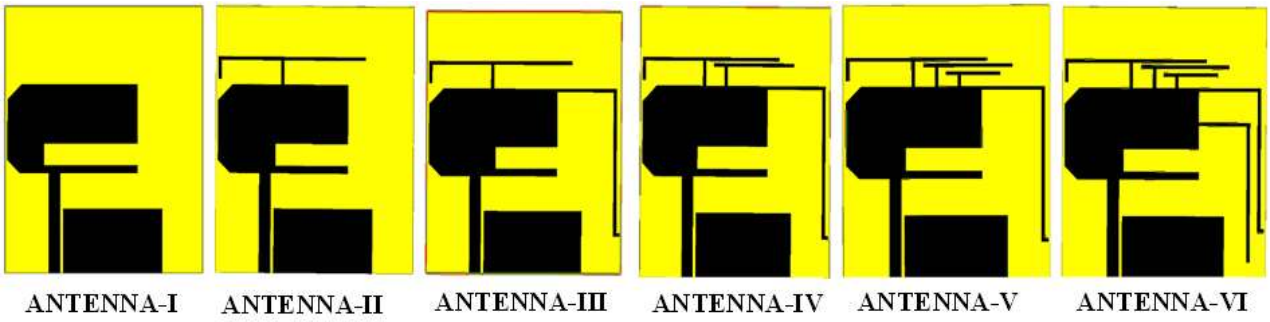

FIGURE 2. Evolution stages of the investigated design

In the second step (Antenna II), due to the addition of F-shaped monopole second mode resonating at 3.45 GHz is achieved to provide LTE band 52 services. Antenna II operates at the two frequencies 3.45 GHz and 5.68 GHz with a decent reflection coefficient of -21.27 dB and -20 dB, respectively as illustrated in Fig. 3.In the third step (Antenna III), an Z shaped monopole is attached to the patch antenna to achieve third resonance at 2.35 GHz to provide LTE band 30 services. Antenna III operates at the three frequencies 2.35 GHz, 3.53 GHz and 5.68 GHz with decent reflection coefficient of -20.3 dB, -22.85 dB and -14 dB, respectively as illustrated in Fig. 3.In the fourth step (Antenna IV), a T shaped monopole is added thus providing fourth resonance at 4.28 GHz to provide radio altimeter services.Antenna IV operates at four frequencies 2.35, 3.5, 4.28 and 5.68 GHz with a decent reflection coefficient of -13.3, -24.7, -18.1 and -31.6, respectively as illustrated in Fig. 3.In the fifth step (Antenna V), another T shaped monopole of shorter length is connected to patch to achieve fifth resonance at 5.2 GHz to provide U-NII-2A band services. Antenna V operates at five frequencies 2.32, 3.47, 4.23, 5.2 and 5.68 GHz with a good reflection coefficient of -17, -14, -22, -12.8 and -26.9 dB, respectively as illustrated in Fig. 3. In the final step (Antenna VI), an inverted L-shaped monopole is added to achieve sixth resonance at 5.2 GHz to provide LTE band 53 services.Antenna VI operates at five 2.35, 2.55, 3.45, 4.28, 5.22 and 5.68 GHz with very small frequency ratios of the values of 1.085, 1.352, 1.24, 1.219, and 1.088 between two consecutive resonant frequencies and a good reflection coefficient of -17.7, -16.3, -19.3, -22.6, -14.3 and -24.7 dB, respectively as illustrated in Fig. 3. Table 2 shows a simulated performance evaluation of the presented antenna under various evolution scenarios. The length of the monopoles (Antennas (II -VI)) are calculated as:

$T_{2.35\ GHz}$ = 18.11 mm (L_4+L_5+L_6)

$T_{2.55\ GHz}$ = 16.7 mm (L_{11}+L_{12})

$T_{3.45\ GHz}$ = 17.5 mm (L_1+L_2+L_3)

$T_{4.28\ GHz}$ = 9.9 mm (L_7+L_8)

$T_{5.2\ GHz}$ = 6.1 mm (L_9+L_{10})

These lengths are roughly one-quarter of the guided wavelength, i.e.,

$$T_{f_r} = \frac{c}{2f_r\sqrt{\varepsilon_{reff}}}$$

where,f_r is the resonance frequency, c = 3 × 10^8 ms^{-1} is the velocity of light in vacuum, and ε_{reff} is the effective permittivity of the substrate, given by:

$$\varepsilon_{reff} = \frac{\varepsilon_r + 1}{2}$$

TABLE II

SIMULATION-BASED PERFORMANCE ANALYSIS OF THE PRESENTED ANTENNA

Configuration	Operating frequency (GHz)	S_{11} (dB)	Bandwidth (GHz)	Bandwidth (MHz)	Bandwidth (%)	Gain (dBi)
Antenna-I	5.68	-25.9	5.6-5.76	160	2.8	1.7
Antenna-II	3.45	-21.27	3.35-3.54	190	5.5	1.2
	5.68	-20	5.6-5.76	160	2.8	2.5
Antenna-III	2.35	-20.3	2.33-2.38	50	2.1	1.47
	3.53	-22.85	3.45-3.63	180	5.1	2.6
	5.68	-14	5.56-5.75	190	3.4	4.8
Antenna-IV	2.35	-13.3	2.33-2.37	40	1.7	1.5
	3.5	-24.7	3.45-3.55	100	2.8	2.0
	4.28	-18.1	4.21-4.37	160	3.7	2.9
	5.68	-31.6	5.59-5.75	160	2.8	4.6
Antenna-V	2.32	-17	2.3-2.35	50	2.1	1.6
	3.47	-14	3.4-3.52	120	3.5	1.9
	4.23	-22	4.17-4.32	150	3.5	2.84
	5.2	-12.8	5.16-5.23	70	1.3	4.2
	5.68	-26.9	5.61-5.75	140	2.5	4.9
Antenna-VI	2.35	-17.7	2.34-2.36	20	0.9	1.6
	2.55	-16.3	2.53-2.59	60	2.3	1.9
	3.45	-19.3	3.37-3.52	150	4.3	2.84
	4.28	-22.6	4.22-4.36	140	3.3	4.2
	5.22	-14.3	5.18-5.25	70	1.3	4.9
	5.68	-24.7	5.62-5.75	130	2.3	5.8

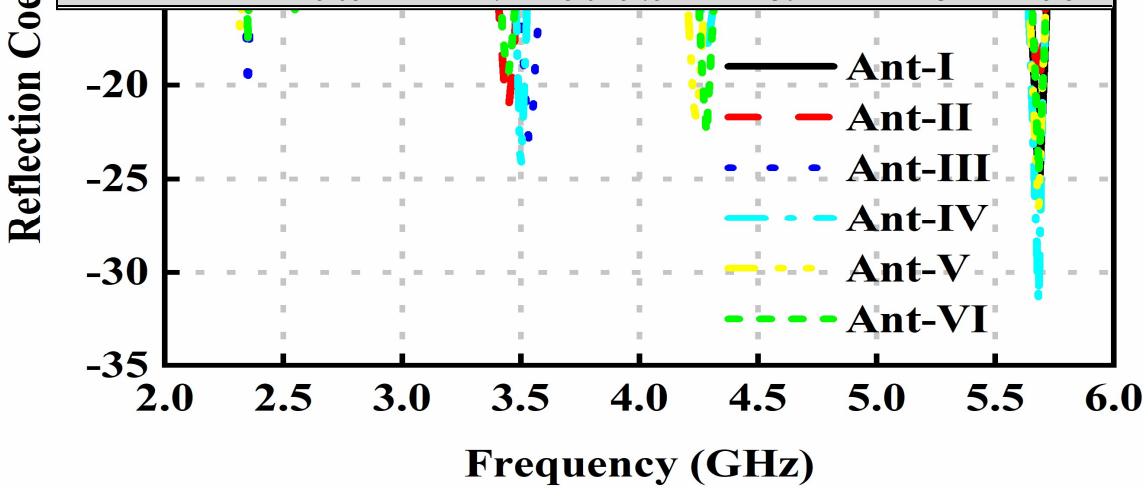

FIGURE 3. Simulated S11 at each step of evolution

III. Frequency reconfigurability

A. PIN diode model

Because of their small size, durability, fast switching speed, and low capacitance and resistance in the OFF and ON states, PIN diode is used to achieve reconfigurability in the investigated design. The equivalent circuit models for the PIN diode in ON and OFF states are depicted in Fig. 4(a). A package inductance L persists in both the ON and OFF states. In the ON state, the equivalent circuit has a low resistance RS, that adds to the insertion loss. The parallel combination of the total capacitance CT and reverse bias resistance Rp in the equivalent circuit for the OFF state adds to isolation. The PIN diode SMP 1320-079 LF from Skyworks Solutions Inc was employed to achieve frequency reconfigurability. From the datasheet of the SMP1320-079 the circuit parameters are L = 0.7 nH, RS = 0.9 Ω, CT = 0.3 pF, and Rp = 3 KΩ. In HFSS simulation, diode is modelled using the Resistance, Inductance, and Capacitance (RLC) boundary by introducing two rectangular sheets in the diode position as illustrated in Fig. 4(b).

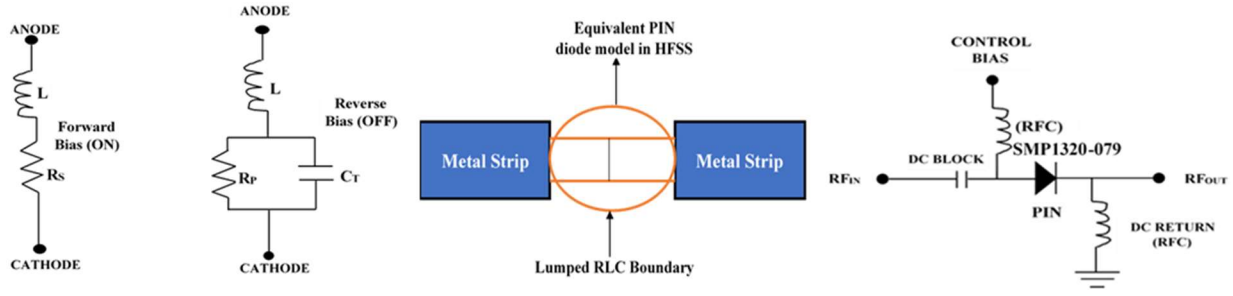

(a) **(b)** **(c)**

FIGURE 4. PIN diode electrical model a) Equivalent model using lumped elements. b) Model in HFSS and c) Biasing circuit

B. Biasing circuit

To accurately bias the PIN diode, some isolation in between the RF signal and DC signal is required. Otherwise, the efficiency of the power control circuit is decreased by the flow of RF current into the output impedance of the power supply. The DC bias supply is isolated from the RF circuits by connecting an RF inductor of 33 nH from coilcraft in series with the bias line, and an RF by-pass capacitor of 10 pF from Murata in series with the RF input as shown in Fig 4(c). The circuit is also wired to 5V regulated supply as shown in Fig 4(c).

IV. Results and Discussion

To justify the HFSS simulation results, the investigated antenna is fabricated, and an antenna model integrated with a biasing circuit is shown in Fig. 5. A calibrated Agilent/HP N9923A 6 GHz Handheld RF Vector Network Analyzer is employed to measure the reflection coefficient. Single PIN diode (D1) is used for possible two modes of operation of the presented antenna.

Catalyst Research Volume 23, Issue 2, September 2023 Pp. 614-630

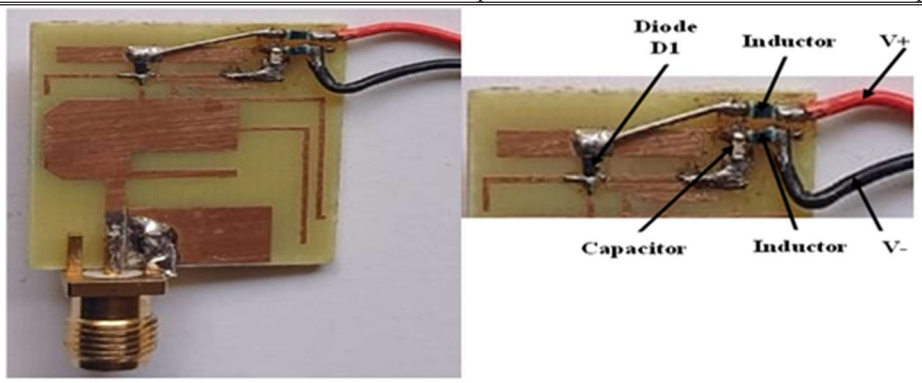

(a)

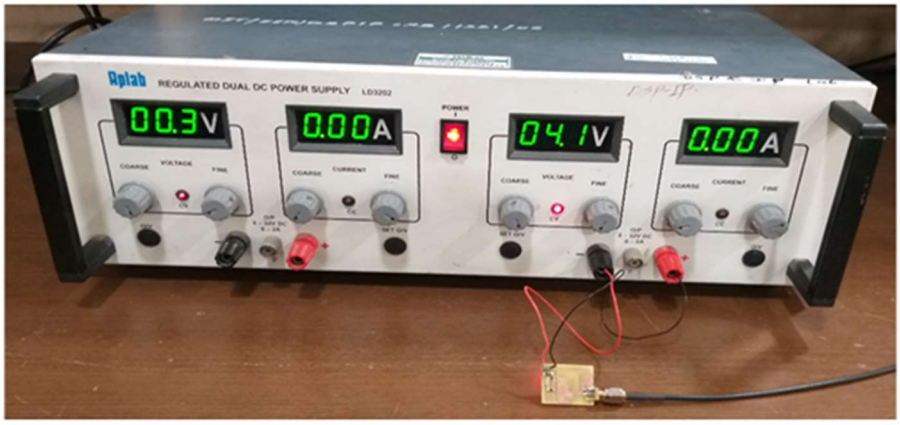

(b)

FIGURE 5. a) Fabricated model of the proposed design integrated with biasing circuit and (b) Experimental setup

A. Mode 1

When the PIN diode (D1) is turned OFF, the proposed antenna operates in Mode 1. Fig. 6 demonstrates the measured and simulated S_{11} characteristics of the investigated antenna in this mode. As illustrated in Fig. 6, in this mode the proposed antenna exhibits hexa-band characteristics with measured $S_{11} < -10$ dB impedance bandwidth of about 2.3 GHz (2.25-2.32 GHz, 3%), 2.5 GHz (2.46-2.52 GHz, 2.4%), 3.35 GHz (3.23-3.45 GHz, 6.6%), 4.4 GHz (4.33-4.47 GHz, 3.2%), 5.3 GHz (5.24-5.36 GHz, 2.3%) and 5.6 GHz (5.53-5.67 GHz, 2.5%)

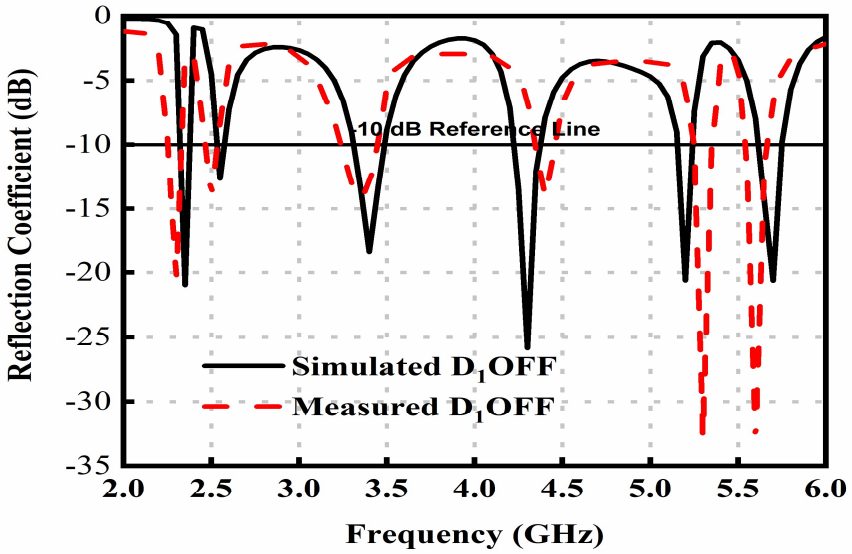

FIGURE 6. Compared S_{11} results of the proposed design for Mode 1

The simulated surface current densities (A/m) for the six resonating frequencies are plotted in Fig 7 to understand better the radiating features of the investigated antenna. Figure 7(a) demonstrates that the maximum current distribution is recognized along the Z shaped monopole at a lower resonant frequency, 2.3 GHz. Figure 7(b) illustrates that at 2.5 GHz, the maximum current distribution is focused along the inverted L-shaped monopole. At the operating frequency of 3.35 GHz, the maximum current distribution is centered along the F-shaped monopole, as depicted in Fig 7(c). At the operating frequency of 4.4 GHz, the surface current is extremely distributed along the T shaped monopole, depicted in Fig 7(d). At the operating frequency of 5.3 GHz, the surface current is extremely distributed along the smaller T shaped monopole, depicted in Fig 7(e). A further finding has been that the surface current distribution is most focused across the bottom part of patch and feed line at 5.6 GHz, as illustrated in Fig 7(f). The operational frequency bands of the investigated antenna in this mode as illustrated from the simulated and measured reflection coefficients can cover six commercial bands of LTE Band 30, LTE Band 53, LTE Band 52, radio altimeter,U-NII-2A, and U-NII-2C, respectively.

B. Mode 2

When the PIN diode (D1) is turned ON, the proposed antenna operates in Mode 2. Fig. 8 demonstrates the measured and simulated S_{11} characteristics of the proposed antenna in this mode.It can be seen from Fig. 8, in this mode the proposed antenna exhibits triple-band characteristics with measured $S_{11} < -10$ dB impedance bandwidth of about 4.35 GHz (4.27-4.43 GHz,3.7%), 5.25 GHz (5.17-5.33 GHz,3%), and 5.65 GHz (5.57-5.72 GHz,2.7%). The proposed antenna in the Mode 2 covers three commercial bands of radio altimeter, U-NII-1 & U-NII-2A and U-NII-2C, respectively.

Catalyst Research Volume 23, Issue 2, September 2023 Pp. 614-630

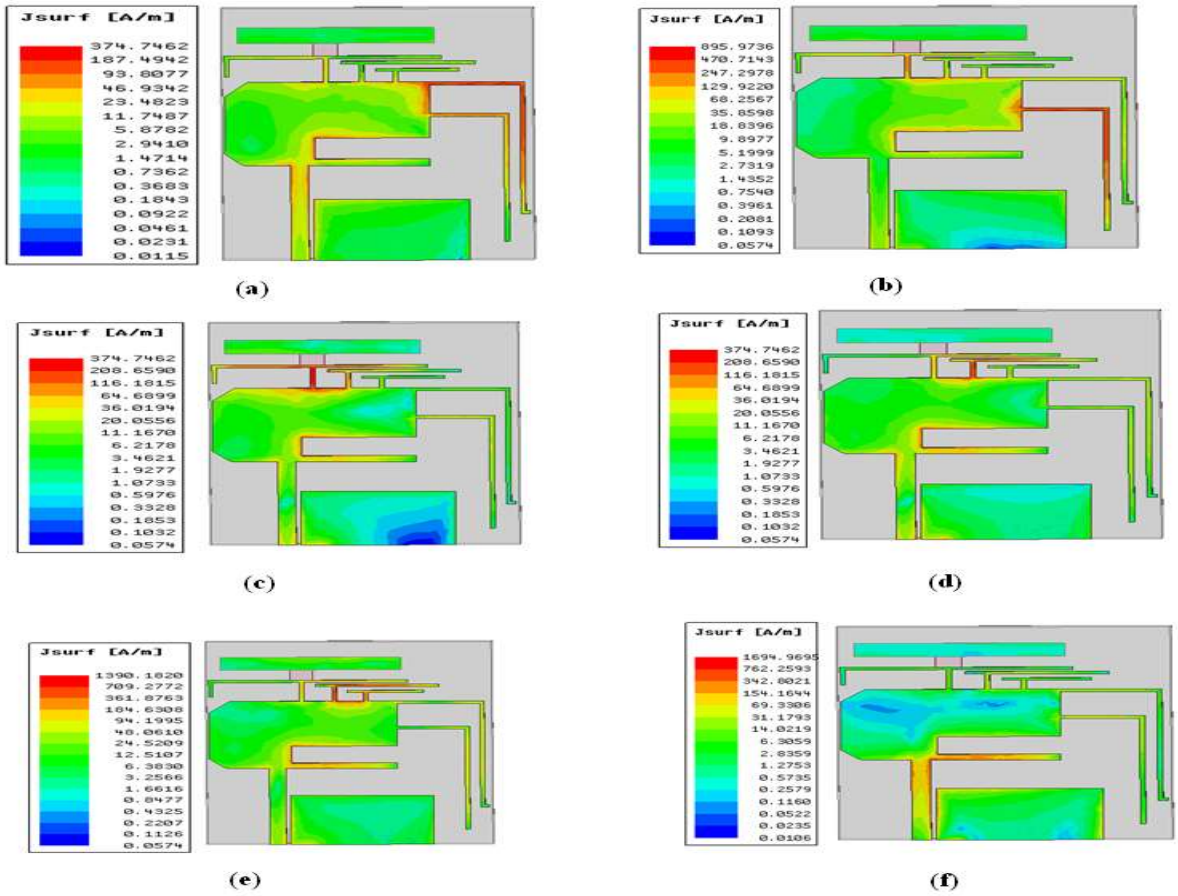

FIGURE 7. Simulated surface current distributions at (a) 2.3 GHz, (b) 2.5 GHz (c) 3.35 GHz, (d) 4.4 GHz, (e) 5.3 GHz and (f) 5.6 GHz.

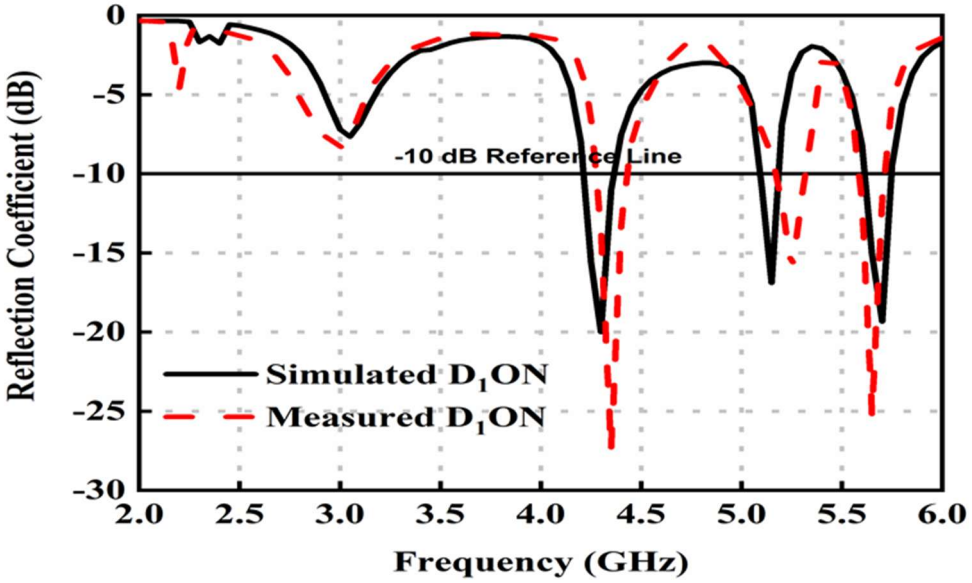

FIGURE 8. Compared S_{11} results of the proposed design for Mode 2

Catalyst Research Volume 23, Issue 2, September 2023 Pp. 614-630

Fig 9 (a) illustrates the set-up to measure S11 using vector network analyzer (VNA), Fig 9 (b) presents the snapshot of VNA for Mode 1 and Fig 9 (c) presents the snapshot of VNA for Mode 2. The proposed antenna's simulation and measurement values are compared in terms of reflection coefficients S11(dB), impedance bandwidth, gain, and the resulting values are illustrated in Table 3.

FIGURE 9. (a) S_{11} measurement set-up using VNA (Model **No: N9923A), (b) Snap shot of VNA screen for Mode 1 and (c) Snap shot of VNA screen for Mode 2**

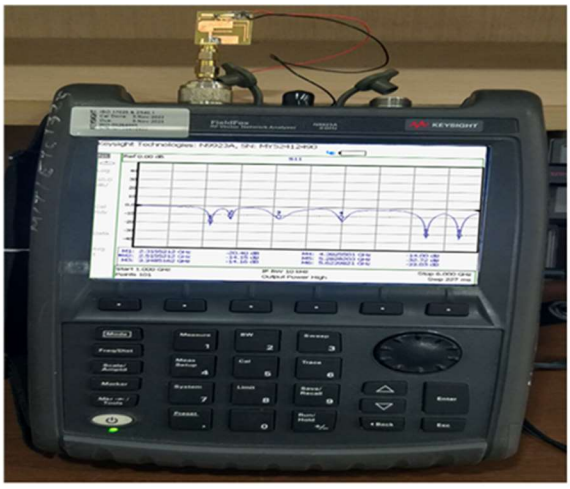

(a)

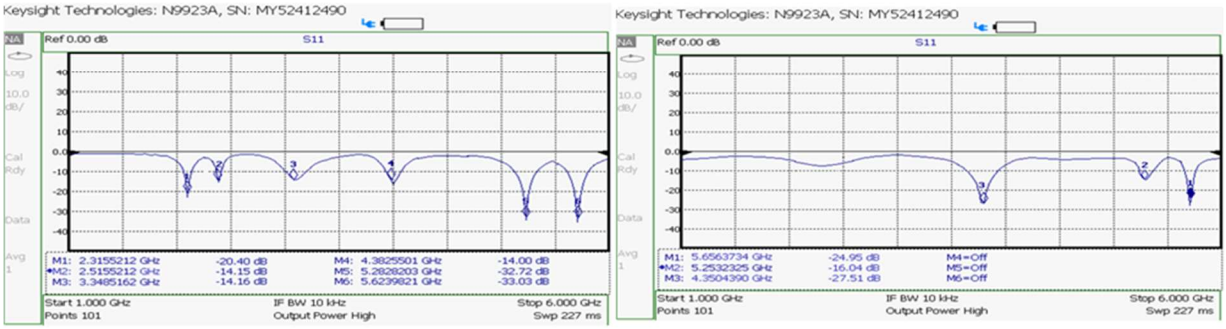

(b) (c)

To further investigate the radiation characteristics of the proposed antenna, 2D E & H plane pattern are examined. In both simulation and measurement modes, the principal plane (E & H) patterns (co/cross-polarization states) are observed, demonstrating a good correlation among these two mode outcomes. The 2D radiation patterns for mode 1 operation are outlined at various wireless communication operating frequencies: 2.3 GHz, 3.35 GHz and 5.6 GHz, respectively as indicated in Figure 10. The investigated antenna has a unidirectional radiation pattern in the E- and H-planes at all operating frequencies.

TABLE 3

POSSIBLE MODES WITH THEIR CORRESPONDING $S_{11,}$ IMPEDANCE BANDWIDTH, and GAIN

Model	Mode	Operational frequency band (GHz)	Reflection coefficient (dB)	Bandwidth (GHz)	Bandwidth (%)	Gain (dBi)
Simulated	1	2.35	-30	2.32-2.38	2.5	1.85
		2.55	-12.6	2.53-2.57	1.6	2.28
		3.4	-18.4	3.31-3.49	5.3	3.46
		4.3	-25.8	4.22-4.37	3.5	2.93
		5.2	-20.6	5.15-5.24	1.7	5.55
		5.7	-20.6	5.62-5.75	2.3	6.26
	2	4.3	-20	4.21-4.36	3.5	2.85
		5.15	-16.8	5.09-5.18	1.8	5.46
		5.7	-19.3	5.61-5.73	2.1	5.98
Measured	1	2.3	-20.4	2.25-2.32	3	1
		2.5	-14	2.46-2.52	2.4	1.5
		3.35	-14.2	3.23-3.45	6.6	2.4
		4.4	-14	4.33-4.47	3.2	2.78
		5.3	-32.7	5.24-5.36	2.3	5.2
		5.6	-33	5.53-5.67	2.5	6.02
	2	4.35	-27.5	4.27-4.43	3.7	2.77
		5.25	-16	5.17-5.33	3	5.13
		5.65	-25.2	5.57-5.72	2.7	5.97

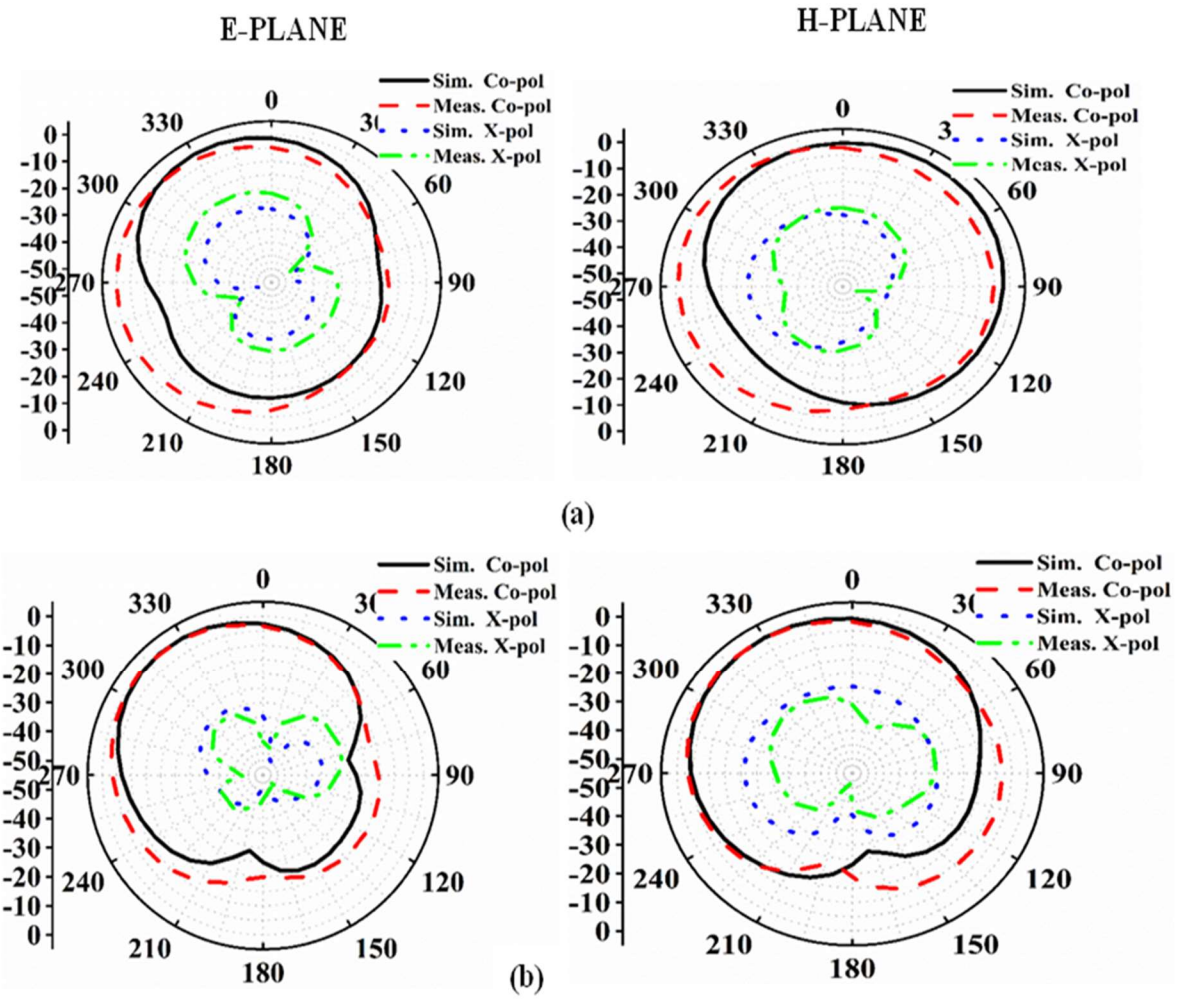

FIGURE 10. Simulated and measured 2D radiation patterns for Mode 1 operation with PIN diode at a) 2.3 GHz, (b) 3.35 GHz, and (c) 5.6 GHz.

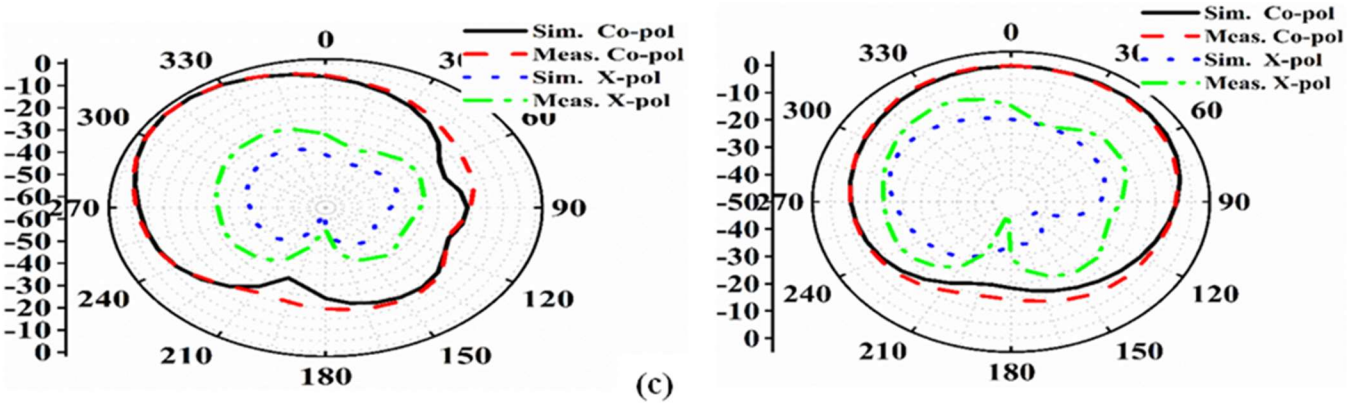

The investigated antenna has simulated gains of 1.85, 2.28, 3.46, 2.93, 5.55 and 6.26 dBi at 2.3, 2.5, 3.35, 4.4, 5.3 and 5.6 GHz and measured gains of 1, 1.5, 2.4, 2.78, 5.2 and 6.02 dBi at 2.3, 2.5, 3.35, 4.4, 5.3 and 5.6 GHz, respectively, as demonstrated in Fig. 11.

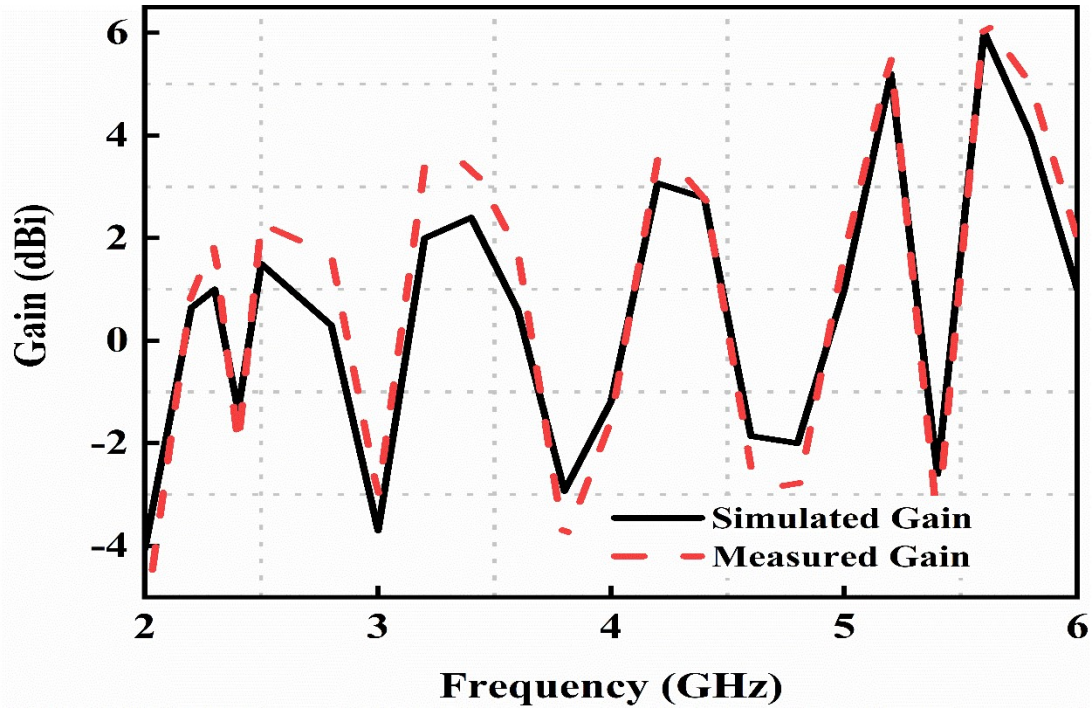

FIGURE 11. Simulated and measured gains of the proposed antenna for Mode 1

The performance comparison between the proposed antenna and the reported existing antennas is shown in Table 4. With frequency band reconfigurability, the proposed antenna operates in six wireless communication operating bands. Furthermore, a single PIN diode is being employed to achieve frequency reconfigurability, lowering the cost of the antenna system. Furthermore, when compared to the antennas listed in Table 4, the investigated antenna has a simpler structure, a larger number of operating bands, and a smaller size

TABLE IV
COMPARISON OF THE PROPOSED DESIGN WITH THOSE IN THE STATE-OF-ART LITERATURE

Ref	Year	Antenna Dimensions (mm^3)	Size Reduction %	No of operating Bands	Minimum Frequency Ratio	Operating Frequencies (GHz)	Frequency Reconfigurability	No of switches	EC Model Analyzed
[9]	2014	120 × 120 × 1.6 23040	96	5	1.17	1.176/1.381/1.575/1.472/1.675	NO	NA	NO
[10]	2019	35 × 35 × 1.5748 1929	62	6	1.059	2.4/3.06/3.34/3.54/4.61/ 5.21	NO	NA	NO
[14]	2019	33.7 × 33.7 × 1.6 1817	60	5	1.18	1.25/1.48/1.8/2.25/2.9	NO	NA	NO
[15]	2019	30 × 30 × 1.6 1440	49	5	1.19	1.01/1.67/2.30/2.92 /3.48	NO	NA	NO
[16]	2018	46 × 39.6 × 1.6 2915	75	6	1.08	2.4/3.8/4.35/ 4.7/5.5/ 6.25	YES	2	NO
[22]	2021	46 × 32 × 1.6 2355	69	5	1.16	1.8/2.1/2.6/3.5/5	YES	12	NO
[23]	2021	44 × 14 × 3.2 1971	63	6	1.06	0.85/0.9/1.6/1.8 1.9/2.1	YES	2	NO
Proposed work	NA	24 × 19 × 1.6 729	NA	6	1.08	2.3/2.5/3.35/4.4/ 5.3/5.6	YES	1	YES

Catalyst Research Volume 23, Issue 2, September 2023 Pp. 614-630

V CONCLUSION

A compact GACS fed frequency reconfigurable hexa-band antenna was presented and investigated. Computer simulations and measurements have shown that the proposed antenna operates at six different frequencies 2.3/2.5/3.35/4.4/5.3/5.6 GHz by switching ON and OFF the PIN diode. The proposed antenna covers six commercial bands of LTE Band 30, LTE Band 53, LTE Band 52, radio altimeter, U-NII-2A, and U-NII-2C. The investigated antenna has simulated gains of 1.85, 2.28, 3.46, 2.93, 5.55 and 6.26 dBi and measured gains of 1, 1.5, 2.4, 2.78, 5.2 and 6.02 dBi at 2.3, 2.5, 3.35, 4.4, 5.3 and 5.6 GHz, respectively.The investigated design yields unidirectional radiation patterns with high reliability and minimal cross-polarization, as well as consistent radiation efficiency/gain and improved impedance matching across all operating wireless communication bands, making it a good choice for inbuilt antennas in multiband wireless portable devices

REFERENCES

1. Balanis, C. A., Antenna Theory Analysis and Design, 4th edition, John Wiley & Sons, 2016.
2. A. Rashidy, A. M, and M. A, “Compact Planar Multiband Antennas for Mobile Applications’, Advancement in Microstrip Antennas with Recent Applications,” InTech, Mar. 06, 2013. https://doi.org/10.5772/52053.
3. Ali, T.; Khaleeq, M.M.; Pathan, S.; Biradar, R.C, “A multiband antenna loaded with metamaterial and slots for GPS/WLAN/WiMAX applications,” Microw. Opt. Technol. Lett., vol 1, pp. 79–85, Nov. 2017. https://doi.org/10.1002/itl2.19
4. Nasimuddin, Z. N. Chen and X. Qing, "Dual-Band Circularly Polarized S-Shaped Slotted Patch Antenna with a Small Frequency-Ratio," IEEE Transactions on Antennas and Propagation, vol. 58, no. 6, pp. 2112-2115, June 2010. https://doi.org/ 10.1109/TAP.2010.2046851.
5. X. L. Bao and M. J. Ammann, "Dual-Frequency Circularly-Polarized Patch Antenna With Compact Size and Small Frequency Ratio," IEEE Transactions on Antennas and Propagation, vol. 55, no. 7, pp. 2104-2107, July 2007. https://doi.org/10.1109/TAP.2007.900271.
6. Kumar, S., Kanaujia, B.K., Khandelwal, M.K. and Gautam, A.K,” Stacked dual-band circularly polarized microstrip antenna with small frequency ratio,” Microw. Opt. Technol. Lett., vol 56, pp. 1933-1937, May 2014. https://doi.org/10.1002/mop.28482
7. Kumar, S., Kanaujia, B., Khandelwal, M., & Gautam, A,” Single-feed circularly polarized stacked patch antenna with small-frequency ratio for dual-band wireless application,” International Journal of Microwave and Wireless Technologies, vol. 8, pp. 1207-1213, Apr. 2015. https://doi.org/10.1017/S1759078715000720
8. Chaurasia, P., Kanaujia, B., Dwari, S., & Khandelwal, M,” Penta-band microstrip patch antenna with small frequency ratios using metamaterial for wireless applications,” International Journal of Microwave and Wireless Technologies, vol. 10, pp. 968-97, Jul. 2018. https://doi.org/10.1017/S1759078718000570

9. M. G. N. Alsath and M. Kanagasabai, "Planar Pentaband Antenna for Vehicular Communication Application," IEEE Antennas and Wireless Propagation Letters, vol. 13, pp. 110-113, 2014. https://doi.org/10.1109/LAWP.2013.2295631.
10. Praveen Chaurasia, Binod Kumar Kanaujia, Santanu Dwari & Mukesh Kumar Khandelwal," Metamaterial based circularly polarized hexa-band patch antenna with small frequency ratios for multiple wireless applications," Journal of Electromagnetic Waves and Applications, vol. 33, pp. 520-540, Jan. 2019. https://doi.org/10.1080/09205071.2018.1561330
11. Hildeberto Jardon-Aguilar, Jose Alfredo Tirado-Mendez, Raul Pena-Rivero & Ruben Flores-Leal, "Multiband–multislot planar antenna based on small loop-radiator," Journal of Electromagnetic Waves and Applications, vol.29, pp. 2066-2079, sep.2015. https://doi.org/10.1080/09205071.2015.1079506
12. C. -X. Mao, S. Gao, Y. Wang and B. Sanz-Izquierdo, "A Novel Multiband Directional Antenna for Wireless Communications," IEEE Antennas and Wireless Propagation Letters, vol. 16, pp. 1217-1220, 2017. https://doi.org/10.1109/LAWP.2016.2628715.
13. Khandelwal, M., Kanaujia, B., Dwari, S., Kumar, S., & Gautam, A, "Triple band circularly polarized compact microstrip antenna with defected ground structure for wireless applications," International Journal of Microwave and Wireless Technologies, vol. 8, pp. 943-953, 2016. https://doi.org/10.1017/S1759078715000288
14. Antara Ghosal, Sisir Kumar Das, Annapurna Das," Multifrequency rectangular microstrip antenna with array of L-slots," AEU - International Journal of Electronics and Communications, Vol. 111, 2019, https://doi.org/10.1016/j.aeue.2019.152890.
15. Daniel, R. Samson. "A CPW-fed rectangular nested loop antenna for penta band wireless applications." AEU - International Journal of Electronics and Communications, vol. 139 2021. https://doi.org/10.1016/j.aeue.2021.153891
16. Chaurasia, Praveen, Kanaujia, Binod, Dwari, Santanu and KHANDELWAL, MUKESH, "Antenna with hexa-band capabilities for multiple wireless applications," Progress in Electromagnetics Research C, vol. 82, pp. 109-122, 2018. https://doi.org/10.2528/PIERC17120602
17. Songnan Yang, Chunna Zhang, H. K. Pan, A. E. Fathy and V. K. Nair, "Frequency-Reconfigurable Antennas for Multiradio Wireless Platforms," in IEEE Microwave Magazine, vol. 10, no. 1, pp. 66-83, February 2009, doi: 10.1109/MMM.2008.930677.
18. Ghanshyam Singh, Binod Kumar Kanaujia, Vijay Kumar Pandey, Deepak Gangwar & Sachin Kumar (2021) Hexa-band pattern reconfigurable antenna with defected ground plane, International Journal of Electronics, 108:11, 1899-1913, DOI: 10.1080/00207217.2020.1870749
19. Y. P. Selvam et al., "A Low-Profile Frequency- and Pattern-Reconfigurable Antenna," in IEEE Antennas and Wireless Propagation Letters, vol. 16, pp. 3047-3050, 2017, doi: 10.1109/LAWP.2017.2759960.

Catalyst Research Volume 23, Issue 2, September 2023 Pp. 614-630

20. Al-Yasir, Yasir & Oguntala, George & Abdullah, Abdulkareem & Husham, M. & Al-Waily, Ramzy & Abd-Alhameed, Raed & Noras, James. (2017). Design of Frequency-reconfigurable Multiband Compact Antenna using two PIN diodes for WLAN/WiMAX Applications. IET Microwaves, Antennas & Propagation. 11. 10.1049/iet-map.2016.0814.
21. Ghaffar, A, Li, XJ, Awan, WA, Nazeri, AH, Hussain, N, Seet, B-C. Compact multiband multimode frequency reconfigurable antenna for heterogeneous wireless applications. Int J RF Microw Comput AidedEng. 2021; 31:e22659 https://doi.org/10.1002/mmce.22659
22. I. Ahmad et al., "A Pentaband Compound Reconfigurable Antenna for 5G and Multi-Standard Sub-6GHz Wireless Applications," Electronics, vol. 10, no. 20, p. 2526, Oct. 2021, doi: 10.3390/electronics10202526.
23. Adnan Ghaffar, Ahsan Altaf, Aayush Aneja, Xue Jun Li, Salahuddin Khan, Mohammad Alibakhshikenari, Francisco Flalcone, Ernesto Limiti, "A Frequency Reconfigurable Compact Planar Inverted-F Antenna for Portable Devices", International Journal of Antennas and Propagation, vol. 2022, Article ID 7239608, 9 pages, 2022. https://doi.org/10.1155/2022/7239608
24. Sreelakshmi, K., Rao, G.S. Reconfigurable Quad-Band Antenna for Wireless Communication. J. Electr. Eng. Technol. 15, 2239–2249 (2020). https://doi.org/10.1007/s42835-020-00492-9